International Journal of Heat and Technology
Vol. 44, No. 1, February, 2026, pp. 115-131
Journal homepage: http://iieta.org/journals/ijht

Transient Thermal Response Analysis of Al_2O_3-Graphene Hybrid Nanofluid-Enhanced Heat Pipes at Varying Inclination Angles and Heat Loads

Soham Joshi*, Kaustubh Kulkarni, Anuj Rathod, Atharv Soni, Pushkar Pawar, Hrithikesh Kolekar

Department of Mechanical Engineering, Dr Vishwanath Karad MIT World Peace University, Pune 411038, India

Corresponding Author Email: soham.joshi3@mitwpu.edu.in

https://doi.org/10.18280/ijht.440110

Received: 10 October 2025
Revised: 22 December 2025
Accepted: 6 January 2026
Available online: 28 February 2026

Keywords:
hybrid nanofluids, heat pipe, inclination angle, electronic cooling, transient thermal analysis

ABSTRACT

In this work, the transient thermal performance of a copper heat pipe containing an Al_2O_3-graphene hybrid nanofluid is investigated, with particular emphasis on the early stages of heat transfer, which are of utmost importance in applications involving rapid heating rates in electronic devices. Formulations of hybrid nanofluids with concentrations of 4%–3%, 3%–2%, and 6%–3% Al_2O_3- graphene were prepared in a water-based fluid at a 50% filling ratio under forced-convection cooling. Experiments were conducted at heat levels of 10-20 W with a step of 5 W, with 0°, 60°, and 90° inclination angles, and transient effects were analysed at a 10-minute post-heating time point. In a comparative assessment against water, the hybrid nano-fluids exhibit improved early transient heat-transfer performance, with lower thermal resistance and lower evaporator temperatures. In this series of experiments, testing at a 60° inclination yielded optimal performance for a hybrid nano-fluid composition of 4%–3%. Taken in a synoptic perspective, this work demonstrates significant promise for the use of hybrid nanofluid heat pipes in efficient transient thermal management applications in contemporary electronic devices.

1. INTRODUCTION

A considerable amount of effort in the field of electronic cooling has focused on developing cooling technologies to meet the demands of steady-state operations. Nevertheless, it is a general observation that electronic devices are deployed in time-variant loading conditions. These include microprocessors (especially those deployed in mobile technology), power-electronic devices (such as insulated-gate bipolar transistors, IGBTs), and high-power semiconductor laser diode arrays (LDAs) [1].

The increasing power and heat dissipation rates in electronic devices have significantly increased heat generation, making heat dissipation a design challenge in recent years. Effective heat transfer in the cooling of CPUs, LEDs, Rectifiers, Transistors, travelling-wave receivers, Audio, and Radio Frequency (RF) amplifiers is essential, as the reliability of these devices depends strongly on operating temperature. The cooling systems of these devices must be efficient to achieve high performance. Approximately 50% of failures of these devices are attributable to temperature-related issues. This proves the requirement for compact cooling systems for these devices. Raising the temperature by 10 ℃ will halve the service life of these devices. Lowering the temperature by 10 ℃ can extend their lifespan by a factor of 2. A transient thermal management system must be used in these devices to ensure their performance [2, 3].

As shown in Figure 1, Heat pipes are passive systems that can transfer heat over long distances without significant temperature loss. Specialists, researchers, and students seeking information on heat pipe science typically spend considerable time browsing archival journals and books on heat pipes. This is among the reasons researchers continue to develop innovative applications of heat pipes [4].

A capillary heat pipe, also referred to as a conventional heat pipe, is a sealed container with a wick structure that lines the inner wall of a tube. The wick is a critical component of the heat pipe, serving as a capillary pump that returns the liquid to the evaporator section. The heat pipe was filled with an appropriate amount of working fluid to saturate the wick. The following describes the operation of a capillary heat pipe: The capillary heat pipe is heated at its evaporator section. The water absorbs heat and evaporates. The vapour then travels to the condenser part due to a higher vapour pressure in the evaporator. The vapour, now hot, condenses to a liquid using the latent heat of vaporisation. The liquid is then sucked by capillary action to the evaporator part of the heat pipe, thus forming a cycle. Capillary heat pipes are most effective due to their two-phase cycle, which enables efficient heat transfer over long distances with minimal temperature drop. They can also maintain a nearly uniform temperature across the surfaces, making them ideal for temperature regulation. However, the critical limitation of these heat pipes is the capillary limit. This occurs when the wick fails to provide sufficient liquid flow to the evaporator, resulting in a markedly elevated, constant rise in evaporator temperature. The conventional capillary heat pipe is widely used in consumer electronics, such as laptops and notebooks, to dissipate heat from processors efficiently. Furthermore, it is used in commercial applications and critical space programs due to its high performance and reliability.

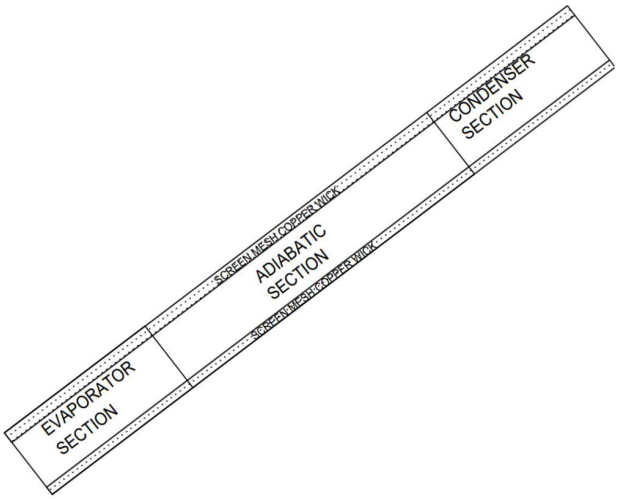

Figure 1. Heat pipe

A heat pipe's thermal characteristics depend on multiple coupled factors, including the working fluid, filling ratio, inclination angle, and heat load. In recent years, nanofluids comprising a specific nanoparticle type and a base working fluid have attracted considerable attention owing to their enhanced thermal conductivity. However, traditional nanofluids have exhibited performance instability, primarily due to nanoparticle agglomeration that settles at the bottom of the heat pipe during operation. To compensate for this drawback, there is a growing interest in hybrid nanofluids that combine two distinct nanoparticle types with an appropriate base working fluid, thereby improving thermal conductivity while maintaining the stability of the working fluid.

This paper examines the transient thermal performance characteristics of a copper heat pipe filled with an Al_2O_3-graphene hybrid nanofluid. Hybrid nanofluids were prepared at volume concentrations of 4%–3%, 3%–2%, and 6%–3% (Al_2O_3-Graphene), using water as the base fluid. The thermal performance of a heat pipe was then measured over a fixed 10-minute post-heating period under different heat loads, with the heat pipe inclined at 0°, 60°, and 90°, at 50% fill ratio, and forced convective cooling. The experimental observations revealed that hybrid nanofluids exhibited superior transient thermal performance relative to water during the initial phase.

Despite extensive research on heat pipes using mono- and hybrid nanofluids, a significant limitation in most studies is the availability of steady-state thermal performance evaluation, which overlooks the transient phenomena during which most electronics fail. Also, most current research considers either the nanofluid combination, the angle of inclination, or the heat load, but not the combination of these factors under transient operating conditions. Furthermore, experimental research on the transient performance of Al_2O_3-graphene hybrid nanofluid-based heat pipes at short time scales is minimal. The novelty of the current study relies upon the evaluation of the transient performance (10 minutes) of a heat pipe considering the combination of the concentration of the hybrid nanoparticles, the angle of inclination, and the heat load, considering thermal resistance as the performance criterion, which fetches significant information applicable to practical electronics involving shorter-time heating effects before achieving a steady-state heat dissipation operation.

The remainder of this paper is organised as follows: Section 2 provides a comprehensive review of the literature on heat pipe cooling, including the effects of working fluid, mono- and hybrid nanofluids, inclination angles, and wick design. Section 3 also explains the method used to prepare Al_2O_3-graphene hybrid nanofluids, including the principles underlying the estimation of their thermophysical properties. Section 4 also describes the preparation of the heat pipe and the cooling system setup, including the instrumentation and testing conditions employed to conduct the transient thermal performance analysis of the heat pipe at different inclination angles and heat inputs. Section 5 also explains the principles of the procedure for estimating the performance characteristics and relevant parameters of the heat pipe described above. Section 6 also offers a comprehensive discussion and analysis of the results, including the effects of inclination angles, heat inputs, and the different compositions of the hybrid fluid. Finally, Section 7 presents the concluding remarks and future work.

2. LITERATURE REVIEW

2.1 Various working fluids in a heat pipe

Han et al. [5] investigated the oscillation characteristics and heat-transfer performance of a closed-loop pulse heat pipe using four different working fluids: deionised water, methanol, ethanol, and acetone. These were tested under various heat inputs (5–100 W) and different filling ratios (20%–95%). The researchers concluded that, for the same filling ratio, a pulse heat pipe charged with a working fluid having a lower boiling point and lower latent heat of vaporisation, such as acetone, was more prone to drying out. Among the thermophysical properties, dynamic viscosity was found to be the most influential, playing a critical role in the start-up of oscillations in the closed-loop pulse heat pipe, particularly at higher heat inputs, provided that no dry-out occurred. Regarding thermal resistance, the performance of different working fluids converged, indicating that the heat-transfer capacity of the pulse heat pipe had reached a maximum. Beyond this point, it isn't easy to achieve significant improvements. This is because, at a certain pulse, the thermal resistance within the tube wall became negligible relative to the external thermal resistance due to air convection.

Mozumder et al. [6] assessed the performance of the heat pipe using different working fluids—water, ethanol, and acetone—based on thermal resistance and the overall heat-transfer coefficient. The filling ratio was varied, and the performance parameters were observed with different liquid inventories at heat loads ranging from 2 to 10 W in 2 W steps. The overall heat-transfer coefficient of the heat pipe increased with increasing heat input for acetone and methanol, whereas the water-filled heat pipe exhibited a nearly constant value. The filling ratio had a minimal effect on the temperature difference across the heat pipe when water and ethanol were used as working fluids. However, for acetone, increasing the filling ratio reduced the temperature difference between the evaporation and condenser sections. When acetone was used as the working fluid, a 100% filling ratio produced the best results, with the smallest temperature difference between the evaporation and condensation areas. In general, filling the heat pipe with more than 85% of its volume with a working fluid showed an improved performance. This includes increased heat transfer coefficients, reduced thermal resistance, and a lower temperature difference between the evaporation and condenser sections.

The choice of working fluid and pressure in a heat pipe depends on its operating temperature range. For instance, water has a critical temperature of 374.1 ℃ and a triple-point temperature of 0.01 ℃, meaning that it can only undergo a phase change within this range. Thus, water is unsuitable for applications outside these temperature ranges. For water to change its phase at a given temperature, the pressure inside the heat pipe must match the saturation pressure at that temperature. For example, to operate at 70 ℃, the pressure must be 31.2 kPa, which is much lower than atmospheric pressure (101 kPa), thereby requiring the heat pipe to operate in a vacuum. If the pressure is maintained at atmospheric pressure, the water will heat without evaporating, thereby reducing the heat-transfer efficiency. Although water is suitable for moderate temperatures, other fluids are required for cryogenic or high-temperature applications. Heat pipes can use fluids that operate from near absolute zero (e.g., helium) to over 1600 ℃ (e.g., lithium). However, practical applications avoid extremes near the critical point to maintain manageable pressures and effective heat transfer. Other factors in choosing a fluid include high surface tension, compatibility with wick materials, and properties such as stability, non-toxicity, availability, and cost.

2.2 Effect of nanofluid as a working fluid

Parametthanuwat et al. [7] investigated the effect of filling ratio (30%, 50%, and 80%) as a function of evaporator length, with condenser coolant flow rates of 1.2, 2.5, and 5 L/min. The five working fluids investigated were water, a water-based silver nanofluid with 0.5 w/v% silver agglomeration, and the nanofluid (NF) mixed with 0.5, 1, and 1.5 w/v% oleic acid (OA) at temperatures of 60 ℃, 70 ℃, and 80 ℃. The experimental results showed that the highest effectiveness, approximately 0.3, and the highest heat flux of approximately 25 kW/m², were achieved at a filling ratio of 50%. The study further concluded that the nanofluid was more effective than water as a working fluid.

Smrity and Yin [8] examined the thermal performance of a three-turn pulsating heat pipe (PHP) using various working fluids, including hybrid nanofluids composed of Aluminium Oxide (Al_2O_3) and Copper (Cu) nanoparticles. They compared this with aluminium oxide monofluid, copper monofluid, and Water. The findings revealed that, with increasing nanoparticle concentration, thermal conductivity also increased. For instance, at 0.1 wt. % and 0.2 wt. % concentrations, it was found that thermal conductivity increased by 10.49% and 15.35%, respectively, compared with water. The activation time of the hybrid nanofluid was shorter than that of other working fluids at comparable heat input, fill ratio, and weight percentage. Moreover, there was a decrease in mean evaporative temperature by 6.25 ℃ in comparison to that of copper oxide mono-nanofluid, 10.5 ℃ in contrast to that of aluminium oxide mon nanofluid, and 22.8 ℃ in comparison to that of distilled water. Furthermore, the hybrid nanofluid exhibited lower thermal resistance than mono-nanofluids. Additionally, at a 60% fill ratio and 0.2 wt.% concentration, it was found that the PHP with Aluminium Oxide-Cu hybrid nanofluid had lower thermal resistance than other mono-nanofluids across a range of heat inputs. The above observations clearly point to the advantages of using hybrid nanofluids, including high thermal conductivity, lower mean evaporative temperature, and lower thermal resistance, making them well-suited for applications such as heat transfer.

Septiadi et al. [3] examined the performance of nanofluids with varying nanoparticle compositions to determine which combination provides the highest thermal conductivity while minimising agglomeration. The material consisted of a mixture of Aluminium Oxide and Titanium Oxide nanoparticles suspended in water at 0.1, 0.3, 0.5, and 0.7 vol.%. The proportions of Aluminium Oxide and Titanium Oxide are set at 75:25, 50:50, and 25:75, respectively. For nanofluid preparation, a magnetic stirrer and an ultrasonic processor are used for 30 min. The testing involved three different methods: determination of KD2 values with high sensitivity, observation of agglomeration, and measurements using UV-VIS Test with HSVC software and applications. The findings indicated that as the vol. % of nanoparticles increased, the level of agglomeration in the nanofluids also increased. The optimal nanoparticulate matter concentration for improving the thermal conductivity of the hybrid fluid was 0.7%. At this concentration, the thermal conductivity relative to pure water increased by 20%–32.5%. Furthermore, the absorbance of the hybrid fluid decreased with increasing storage time. Therefore, the experiment demonstrated that the conductivity and performance of the hybrid fluid can be improved by increasing the nanoparticle concentration.

In experimental and numerical investigations of the effect of hybrid nanofluids in pulsating heat pipes (PHPs) conducted by Zufar et al. [9], considerable improvements in the thermal performance of PHPs using the hybrids were observed relative to water. The hybrids had shorter startup pulsation times and required less heating power to initiate the process across all liquid filling ratios. The average evaporator temperature for heat rates above 30 W was consistently lower for the hybrids than for water, indicating greater suitability at higher power levels. Among the fluids investigated, the SiO_2–CuO hybrid exhibited the lowest thermal resistance due to its higher thermal conductivity and viscosity. The Al_2O_3–CuO had the highest viscosity, although it had the highest thermal conductivity. This underscored the importance of viscosity in matching thermal conductivities to improve the performance of PHPs. The optimal filing ratio for the working fluids, including water, was 60%. The simulation results attested the physical assertion that dryness or dry-out can only occur in water at a filling ratio of 50% with a heat rate of 100 W for dry-out to take place for water in PHPs when the simulation approach in the research was correct and accurate, with a proximity to the experimental conduct and former research findings. This study focused on the performance of a PHP, a passive cooling technology used in thermal management systems, using a nanofluid composed of deionised (DI) water and silver nanoparticles at a 0.1% by volume concentration. The PHP was built from scratch, with temperature measurements using thermocouples in the evaporator and condenser sections and pressurisation measurements using pressure transducers. The design included cartridge heaters in the evaporator section as the heat source, while a chiller was used in the condenser section as the cooling source. Before testing nanofluids containing silver nanoparticles, the system was tested with deionised water alone. The three designed heat inputs of 61 W, 87 W, and 119 W with fill ratios of 30%, 40%, 50%, 60%, and 70% were used in fifteen tests for both nanofluids. Thermal performance was estimated from the computed overall thermal resistance. The findings showed improved PHP performance in 16 of the 15 tests, with the highest performance observed at powers of 61 W and 87 W; however, no improvement was observed at 119 W. This can

be attributed to increased subcooling in the condenser section due to the nanofluid's higher thermal conductivity. There was no significant performance improvement in the evaporator section despite the use of nanofluids, owing to the dominance of vapour. For future studies, other nanofluids, such as ionic liquids, could be investigated as working media, and varying concentrations could be analysed to improve the overall efficiency of PHP [10].

In the study of Sadeghinezhada et al. [11], a systematic experimental study aimed at developing an organic, stable graphene nanoplatelet (GNP) nanofluid and evaluating its performance in heat pipe systems. In the survey, water-soluble GNPs were synthesised via covalent functionalization with the diazonium salt (DS) or with the DS of sodium 4-aminoazobenzene-4-sulfonate. This approach helped increase the stability of the nanoparticles in water. An increase in dispersion stability, along with effective functionalization, was observed in the study. Additionally, experimental results showed that the surface-modified nanoparticles increased the thermal conductivity in the base fluid by 17%. Moreover, the DS-functionalized GNPs exhibited good stability, with only a 16% increase over 480 hours. However, the dispersion became stable up to 840 hours. Furthermore, at a nanoparticle concentration of $\Phi = 5\%$, the versatile nanofluid exhibited a 105% increase in effective thermal conductivity and a 26.4% reduction in thermal resistance. However, the surface temperature of the heat pipe became negative beyond the initial point at a 30% filling ratio. Then, the temperature increased at a 40% filling ratio. However, at 60%, the temperature was positive. Moreover, the maximum average heat-transfer coefficient was observed at the optimum inclination angle of 50°. This was observed due to improved nucleate boiling heat transfer. In the study, at angles between 50 ° and 70°, the thermal resistance values were indicative of a 50° angle. Overall, the study identified the potential of DS-functionalized GNP nanofluids in heat pipes as an effective working medium to enhance heat-transfer capacity.

Rama Narasimha et al. [12] analysed the transient characteristics of a pulsating heat pipe (PHP), with emphasis on experimental methods. The transient temperature variations were analysed using the Fast Fourier Transform (FFT) to determine the Power Spectral Density. Based on experimental analysis, a periodic variation in evaporator wall temperature was observed. Furthermore, among the fluids tested, acetone exhibited the smallest evaporator-to-condenser temperature difference relative to water, ethanol, and methanol. Ethanol exhibited the highest wall temperatures. The experimental analysis revealed that a single-loop pulsating heat pipe can operate at standard pressure. The experimental oscillation cycle counts were consistent with the flow-visualisation analysis. Based on transient analysis, acetone was identified as a well-suited fluid for a pulsating heat pipe. Further, the single-loop pulsating heat pipe performed well at standard pressure operation.

2.3 Effect of the Inclination angle of the working of heat pipes

Mahdavi et al. [13] investigated the thermal performance of a cylindrical copper water heat pipe. They analysed the effects of the input heat rate, the gravitational orientation of the incline angle, and the amount of working fluid in the heat pipe on the temperature distribution and the equivalent thermal resistance of the heat pipe at inclinations of 0°, 60°, and 90°. It was observed that the heat pipe exhibited higher thermal resistance at higher input heat rates due to the reduced fluid volume. Moreover, greater amounts of the filled liquid within the heat pipe increased the thermal resistance because the liquid interferes with the evaporation/condensation processes. The values of the inclination angles had little effect on the heat pipe's resistances at gravity-assisted positions. However, at positions that counteract gravitational forces, higher inclination angles led to poorer performance of the heat pipes than at horizontal positions. Furthermore, liquid retention within the evaporation section of heat pipes significantly affects their performance.

Zhang et al. [14], in their work, investigated a flat-plate heat pipe that used acetone, ethanol, and a one wt % Al_2O_3-water-based nanofluid as the working fluids at fill ratios of 30%, 45%, 60%, and 80% and at heat loads of 15 W, 30 W, 45 W, and 60 W with experiment settings of 0°, 30°, 60°, and 90° inclination angles. In this work, a fill ratio of 60% exhibited the lowest thermal resistance of 2.5 $°C \cdot W^{-1}$, outperforming fill ratios of 30%, 45%, and 80%. Inclination, in particular, showed the best performance, with the heat transfer coefficient increasing by approximately 90.8% as the inclination varied from 0 to 60°, owing to gravity-assisted condensate flow. As the inclination approached 90°, the heat transfer coefficient decreased by approximately 7.2%. A partial dry-out condition was observed at a 30 W heat load. In all cases, the use of a 1 wt% Al_2O_3-water-based nanofluid yielded lower thermal resistance and better overall thermal performance than those obtained with acetone and ethanol.

Veerasamy and Dharini [15] examined the effect of graphene nanofluid on the thermal performance of a heat pipe (HP) compared with deionised water, focusing primarily on the impact of inclination angle. Experiments were carried out at a constant heat input of 40W, with inclination angles of 0°, 45°, and 90°, and a 50% fill ratio. The critical thermal values, such as thermal resistance, the temperature difference between the evaporator and condenser, and the effective thermal conductivity, were examined to assess performance. It was concluded that, for higher inclination angles, the heat pipe efficiency increases, whereas the 90° position exhibited the lowest thermal resistance and the highest thermal conductivity. The 0° position, in contrast, showed the highest thermal resistance, indicating the lowest transport capability.

The experiments analysed the effect of the inclination angle on a cylindrical phase change material (PCM) system, employing various heat-transfer mechanisms to improve its performance. The PCM system was designed with a base copper disk, a heat pipe (HP) or rod, and an additional component made of aluminium foam or foil. The test conditions covered six configurations and a total of twenty-eight test cases to determine effects during both melting and solidification. The analysis of results confirmed that orientation factors were ineffective during solidification due to the prevailing convective heat-transfer mechanisms in the tests, except in the HP-Foil PCM test setup. However, performance differences attributable to inclination were attributed to the HP operating at its capillary limit, particularly when the evaporator was placed on top of the condenser. In contrast, melting performance depended on natural convection effects, with inclination factors that, for the HP-PCM, Rod-PCM, and PCM test cases, led to faster melting than their horizontal-orientation configurations, resulting in higher liquid fractions. The Foil-PCM and HP-Foam-PCM systems showed negligible dependence on system orientation,

maintaining consistent performance. It should also be noted that among the systems, the HP-Foil-PCM system recorded the most notable improvements, including a ninefold increase in melting rate and reductions in PSC solidification and melting times to 3% and 12%, respectively, compared with those of a non-enhanced PCM. These findings indicate that a combination of heat pipes and aluminium foils or foams constitutes an effective heat augmentation system that is independent of system orientation [16].

Alammar et al. [17] conducted numerical analyses using the developed CFD model. They demonstrated the effects of various fill ratios and inclination angles on the performance of the Two-Phase Closed Thermosiphon (TPCT). The model's validity was verified by comparing the data with experimental results from other studies, yielding only 4.2% deviation in wall temperature, 8.1% deviation in the thermal resistance ratio at 65% fill ratio, and 1.3% deviation in the inclination angle. The findings show that the TPCT results in heat-transfer limitations at the lowest fill ratios, such as 25% and 35%, due to insufficient liquid mass, which increases evaporator wall surface temperatures with increasing heat input. The best performance, however, was achieved with a 65% fill ratio and a vertical TPCT inclination angle of 90°. The worst performance was achieved with the 25% fill ratio and a 10° TPCT inclination angle, owing to the combined effects of reduced liquid mass and the unfavourable TPCT inclination angle. The current study clearly demonstrates that the appropriate liquid mass substrate and near-vertical TPCT inclination angles improve heat transfer, achieving the best TPCT performance at a 65% fill ratio and a 90° TPCT inclination angle.

Nazarimanesh et al. [18] investigated the effects of the inclination angle, nanoparticle concentration, and entrance power on a flat-plate heat pipe filled with silver nanofluids. The experimental research used ethanol and Deionised water as working fluids, containing silver nanoparticles at concentrations of 10 ppm, 15 ppm, and 1000 ppm, and volumetric fractions of 0.1%, 0.005%, and 0.001%, respectively. The angle of inclination ranged from -90 ° to +90°, and the entrance power ranged from 10W to 40W. Furthermore, it investigated the effect of cooling-fluid temperatures ranging from 20 ℃ to 40 ℃. The results showed that a 50 ppm silver nanofluid solution exhibited the most significant improvement among the concentrations tested. The results also showed that, at 50 ppm, the lowest thermal resistance was observed at a 30° angle of inclination. The experiment demonstrated a 40% reduction in thermal resistance when a 40 W input power and a 40 ℃ cooling-fluid temperature were used. Further experiments showed that as the entrance power increases, the fluid viscosity decreases sharply, thereby reducing thermal resistance. For an inclined angle, a +90° angle produced a convergent flow between evaporation and condensation, thereby promoting efficient fluid return and heat transfer. On the other hand, a −90° angle produced a divergent force, thereby degrading heat transfer. The finding also shows that at an angle of +90°, a substantial improvement is achieved; hence, using an optimised angle as part of the optimised parameter set is necessary to achieve significant gains.

2.4 Effect of wick structure in heat pipe

Mwaba et al. [19] work on the effect of wick geometry on heat pipe performance. In this work, they emphasised the development of a wick geometry that ensures high capillary pressure and low fluid-flow resistance. Microscopic and macroscale geometric designs of the wick were tailored to enhance heat pipe performance. Three wick designs were numerically analysed: a 100-mesh copper screen wick [19], a sintered copper wick, and a composite wick combining copper screen mesh and sintered copper [20]. The study shows that heat pipe performance depends significantly on the geometric design of the wick material. Among the three designs selected, the composite wick with a combination of coarse and fine pores exhibited the best performance under the tested conditions. It is noted that this geometric design of the composite wick can increase heat pipe performance by up to a factor of two. Additionally, although Cengal [21] exhibits better performance than the other designs, a sudden transition in its geometry can impair optimal heat pipe performance, as indicated by computer simulations.

The previous study conducted experimental and numerical analyses to demonstrate the influence of flat heat pipe wick geometry on thermal performance. The numerical analysis was performed to illustrate the impact of wick porosity on heat pipe performance, including cases that could not be experimentally tested. A comparative analysis was conducted to evaluate the thermal performance of an electronic component cooled by a heat pipe, a copper block, and an open-heat-pipe design. The analysis revealed that, under forced-convection conditions, Heat Pipe A with mesh and powder was more efficient than the copper block and other heat pipe designs. Under free-convection conditions, however, the copper block was the most efficient design. The analysis also confirmed a variation of approximately 19% in temperature, which depended on the heat pipe wick design. The results also confirmed that an increase in porosity contributed to the rise in the heat pipe's temperature and a decrease in its pressure. The analysis compared different wick geometries and confirmed that, at high temperatures, a rectangular-groove design was superior to the wrapped-screen and packed-sphere designs. According to de Iverson et al. [22], more efforts have been made to develop micro- and nano-heat pipes with high efficiency. The authors of this study analysed the efficiency of heat pipes with micro- and nanowick structures. The analysis was explicitly focused on demonstrating the efficiency of wick capillary performance using a bubble-point measurement and a PMI bubble-point apparatus. The results of this experiment confirm a high potential for errors in measuring the efficiency of capillary performance in wicks with tiny pores. It is argued that the bubble point measurement technique is among the simplest and fastest. However, this technique also has associated errors. The authors argued that this technique yields information on the minimum capillary pressure, which may not accurately reflect efficiency, particularly when pore diameters vary widely. A narrow variation of pore diameters is, however, considered to confirm the efficiency of wick performance. The authors attempted to confirm the efficiency of the measurement technique by using a fine-wire mesh screen. The measured pore radii showed minor deviations, all of which were well within one standard deviation of the predicted value, indicating the accuracy of the testing process. In addition to the bubble-point testing method, a four-step wick-sample preparation technique was established to facilitate the bubble-point testing. This technique involved using a disc with a central hole filled with wax, which was subsequently removed by burning during sintering. This method enabled the wick pattern to be attached to the disc

without applying excessive mechanical force. When expected deviations in capillary action are considerable across the sample, multiple holes can be drilled into the disc to enable more general analysis. Analysis of a copper wick identified a significantly smaller average pore diameter than previously reported by other authors, including Chi. This size difference was correlated with factors such as particle size, interparticle necking, and porosity. In addition, the work proposed a novel technique to visualise the fluid's saturation processing within the wick design. Using a fluorescent dye, a UV light source, a UV-filter camera, and image-processing techniques enabled analysis of the dye front's migration over time. This saturation-illustration technique for the designed wick structure enabled identification of the capillary and permeability properties of the structure. This makes the technique a beneficial analysis method [23].

Iverson et al. [22] stated experimentally that it can be seen the most prominent heat transport mechanism within the wick has been the conversion of heat energy to the latent heat of vaporisation. This indicates that the higher the input power, the higher the heat utilisation rate during conversion and the lower the heat conduction rate through the solid portion. This not only increases heat-transfer efficiency but is also noteworthy because the sintered copper powder has the same grain structure yet performs equally well despite being placed upright. The sintered copper powder can efficiently dissipate heat fluxes up to 20 W/cm² without drying out, indicating superior capillary and heat-transfer performance of the fluid and wick. The thermal conductivity of the wick was observed to be approximately three times higher than that of pure copper, signifying the high efficiency of the phase change mechanism".

We selected Al_2O_3 because metal oxide nanoparticles (e.g., Al_2O_3, CuO) exhibit superior chemical inertness but relatively low thermal conductivity. This limitation is effectively addressed by incorporating graphene nanoparticles, as metallic particles (e.g., Ag, Cu, Au) possess high thermal conductivity but lower chemical stability. Consequently, the combination of Al_2O_3 and graphene allows these materials to complement each other effectively [21]. Several studies have reported that graphene-based nanofluids can reduce thermal resistance by up to 83.6%, resulting in a nearly 105% increase in thermal conductivity [23]. Although heat pipe efficiency is strongly influenced by filling ratio, with the effect varying with inclination angle and working fluid, a filling ratio of 50 was selected in this study, as it is more effective for horizontal orientation when water is used as the base fluid (5). Heat pipe performance is also highly dependent on the inclination angle, and the existing literature indicates that gravity-assisted orientations are more effective. To examine this effect, inclination angles of 0˚ (horizontal), 60˚, and 90˚ (vertical) were selected (6)(3). The thermal conductivity and overall performance of hybrid nanofluids have been observed to improve with increasing nanoparticle volume fraction (12). Considering the high thermal conductivity of graphene nanoparticles and the high stability of Al_2O_3, an optimal balance between nanoparticle volume fractions was explored across different inclination angles and heat loads. Accordingly, hybrid nanofluid concentrations of 4%–3%, 3%–2%, and 6%–3% Al_2O_3–Graphene were chosen for this investigation. In this work, the thermal resistance of the heat pipe is used as the primary parameter to select the most suitable heat pipe configuration for a given inclination angle and nanoparticle concentration.

The reviewed literature indicates that while hybrid nanofluids have shown promise in enhancing heat pipe performance, a clear gap remains in understanding their transient thermal behaviour under combined variations in inclination angle and heat load. Most studies emphasise steady-state metrics or long-duration operation, which may not accurately represent real electronic startup conditions. The present study addresses this gap by experimentally focusing on short-duration transient response using Al_2O_3–graphene hybrid nanofluids, thereby extending existing knowledge toward more application-relevant thermal management scenarios.

3. EXPERIMENTATION DETAILS

3.1 Preparation method

Al_2O_3 and Graphene nanoparticles were bought from Shilpent. For the synthesis of the hybrid nanofluid, graphene particles and Al_2O_3 nanopowders are initially blended in a predetermined ratio using a mortar and pestle to achieve a uniform mixture. The powdery mixture is then gradually infused into de-ionised (DI) water using a magnetic stirrer or a glass stirrer to achieve a uniform mixture in about 15–30 minutes. Following stirring, the mixture is placed in an ultrasonic bath to disperse particles uniformly, with a 20-minute on/5-minute off cycle for 1 hour. To prevent overheating, ice packs or chilled water are placed around the beaker to keep the bath temperature below 40 ℃ during sonication. The nanofluid is used immediately after preparation, maintaining stability for approximately 2–4 hours. If slight sedimentation occurs, gentle swirling or brief re-sonication is performed before use. Hybrid nanofluids with 4%–3%, 3%–2%, and 6%–3% (Al_2O_3- graphene by volume) were prepared using water as the base fluid. The thermophysical properties of Al_2O_3 and graphene nanoparticles used in this study are presented in Table 1. Table 2 shows the thermophysical properties of graphene/water mono-nanofluids at different volume concentrations.

Table 1. Thermophysical properties of nanoparticles

Thermophysical Properties	Al_2O_3	Graphene
Density (kg/m^3)	3970	2250
Specific heat (j/kgk)	765	710
Thermal conductivity	40	3000

Table 2. Thermophysical properties of mono-nanofluids

Graphene/Water Mono Nanofluid				
Volume %	Thermal Conductivity	Viscosity	Specific Heat	Density
0	0.6132	0.001002	4179	998
2	0.722749	0.000485	4033.97	1025
3	0.75126	0.000436	3960.44	1037.5

Thermophysical Properties of Al_2O_3 and Graphene Nanofluid are calculated using the following empirical formulae.

Effective density of nanofluid:

$$\rho_{eff} = \rho_b(1 - \varphi_{np}) + \rho_{np}\varphi_{np} \quad (1)$$

where, ρ_{eff} is the effective density of nanofluid, φ_{np} is the volume percentage of the nanoparticles, and ρ_{np} is the density of the nanoparticle.

Effective thermal conductivity of nanofluid:

$$\kappa_{eff} = \frac{\kappa_b[\kappa_{np} + 2\kappa_b - 2\varphi_{np}(\kappa_b - \kappa_{np})]}{\kappa_{np} + 2\kappa_b + \varphi_{np}(\kappa_b - \kappa_{np})} \quad (2)$$

where, κ_{eff} is the thermal conductivity of the nanofluid, φ_{np} is the volume percentage of the nanoparticle, κ_b is the thermal conductivity of the base fluid, and κ_{np} is the thermal conductivity of a nanoparticle.

Adequate specific heat of nanofluid:

$$c_{peff} = \frac{(1 - \varphi_{np}) \times \rho_b c_{pb} + (\varphi_{np} \times \rho_{np} c_{pnp})}{\rho_{eff}} \quad (3)$$

where, c_{peff} is the specific heat of the nanofluid, c_{pb} is the specific heat of the base fluid, and c_{pnp} is the specific heat of a nanoparticle.

Effective Viscosity of Nanofluid:

$$\mu_{eff} = (1 + 2.5\varphi_{np})\mu_b \quad (4)$$

where, μ_{eff} is the effective viscosity of nanofluid, φ_{np} is the volume percentage of the nanoparticles, and μ_b is the viscosity of the base fluid. The thermophysical properties of the Al_2O_3/water nanofluid at different volume concentrations are presented in Table 3.

Table 3. Thermophysical properties of AL_2O_3/ water nano-fluid

AL_2O_3/Water Mono Nanofluid				
Volume %	**Thermal Conductivity**	**Viscosity**	**Specific Heat**	**Density**
0	0.613	0.001002	4179	997.1
3	0.74147	0.00485	3812.664	1063.289
4	0.7749377	0.000543	3699.14	1093.152
6	0.8328	0.000686	3489.75	1152.878

3.2 Thermophysical properties of Al2O3-nano-fluid

The thermophysical properties, such as density, viscosity, and thermal conductivity, increase with nanoparticle concentration, whereas specific heat decreases. Since the thermal conductivity of nano-sized particles is significantly better than that of the base fluid, the interaction between nanoparticles and the base liquid intensifies at higher concentrations. This interaction helps enhance the thermal conductivity of the hybrid nanofluid (HyNF). Viscosity increases with concentration due to stronger cohesive forces between like and unlike molecules. However, contrary to the previous observations, some studies report a slight increase in specific heat with concentration [1].

3.3 Thermal-physical characteristics of Al_2O_3-graphene/water hybrid-nanofluids

Table 4 summarizes the thermophysical properties of the Al_2O_3–graphene/water hybrid nanofluid used in the present study.

Table 4. Thermophysical properties of Al_2O_3-graphene/water hybrid nanofluid

Al_2O_3-Graphene/Water Hybrid Nanofluid				
Volume %	**Thermal Conductivity**	**Viscosity**	**Specific Heat**	**Density**
4-3%	0.818486	0.001975	3945.26	1150.87
3-2%	0.77321	0.001373	4012.1002	1110.417
6-3%	0.8655	0.001262	3878.9706	1208.53

3.4 Thermophysical properties of Al_2O_3-Graphene Nanofluid are calculated using the following empirical formulae

Effective Density of Hybrid Nanofluid:

$$\rho_{hnf} = \phi_{np1}\rho_{np1} + \phi_{np2}\rho_{np2} + (1 - \phi_{hnp})\rho_{bf} \quad (5)$$

where, ρ_{hnf} is the effective density of hybrid nanofluid, ϕ_{np1} is the volume percentage of nano particle 1, ρ_{np1} is the density of the nanoparticle 1, ϕ_{np2} is the volume percentage of the nano particle two and ρ_{np2} is the density of the nanoparticle 2, ϕ_{hnp} is the volume percentage of the hybrid nanoparticle and ρ_{bf} is the density of the base fluid.

Effective Volume percentage of Hybrid Nanofluid:

$$\phi_{hnp} = \phi_{np1} + \phi_{np2}$$

where, ϕ_{hnp} is the effective volume percentage of hybrid nanofluid, ϕ_{np1} is the volume percentage of the nano particle 1 and ϕ_{np2} is the volume percentage of the nano particle 2.

Adequate Specific Heat of Hybrid Nanofluid:

$$Cp_{hnf} = \frac{\phi\rho_{np1}Cp_{np1} + \phi\rho_{np2}Cp_{np2} + (1 - \phi_h)Cp_{bf}}{\rho_{hnf}} \quad (6)$$

where, Cp_{hnf} is the effective specific heat of the hybrid nanofluid, ϕ_{np1} is the volume percentage of nano particle 1, ϕ_{np1} is the volume percentage of nano particle 1, ρ_{np1} is the density of the nanoparticle 1, ϕ_{np2} is the volume percentage of the nano particle two and ρ_{np2} is the density of the nanoparticle 2, ρ_{hnf} is the density of the hybrid nanofluid, Cp_{bf} is the specific heat of the base fluid.

Effective Thermal Conductivity of Hybrid Nanofluid:

$$= k_{bf}\left(\frac{\left(\frac{k_{np1}\phi_{np1} + k_{np2}\phi_{np2}}{\phi_{np1} + \phi_{np2}} + 2k_{bf}\right) - 2(\phi_{np1} + \phi_{np2})\left(k_{bf} - \frac{k_{np1}\phi_{np1} + k_{np2}\phi_{np2}}{\phi_{np1} + \phi_{np2}}\right)}{\left(\frac{k_{np1}\phi_{np1} + k_{np2}\phi_{np2}}{\phi_{np1} + \phi_{np2}} + 2k_{bf}\right) + (\phi_{np1} + \phi_{np2})\left(k_{bf} - \frac{k_{np1}\phi_{np1} + k_{np2}\phi_{np2}}{\phi_{np1} + \phi_{np2}}\right)}\right) \quad (7)$$

where, k_{hnf} is the thermal conductivity of the hybrid nanofluid, ϕ_{np1} is the volume percentage of nano particle 1, ρ_{np1} is the density of the nanoparticle 1, ϕ_{np2} is the volume percentage of the nano particle two and ρ_{np2} is the density of the nanoparticle 2, ϕ_{hnp} is the volume percentage of the hybrid nanoparticle and κ_{bf} is the thermal conductivity of the base fluid.

3.5 Heat pipe details and experimental research

The heat pipe was made of copper, as shown in Figure 2 and Figure 3, with a screen mesh serving as the wick structure. A single 40-mesh layer was used for the screen mesh. Graphene-water nanofluid, Al_2O_3-graphene water nanofluid, and water were used as working fluids in the HP. The evaporator, adiabatic, and condenser sections of the heat pipe each have lengths of 50 mm, 100 mm, and 150 mm, respectively.

For temperature measurement, 4 Thermocouple sensors were mounted on the heat pipe wall surfaces, and two were placed inside the pipe at the evaporator inlet and condenser outlet, respectively. Figure 3 shows the temperature-sensor distribution along the length of the heat pipe. The experimental setup consists of a variac, a digital wattmeter, a mica heater, a temperature scanner data logger, and a cooling fan. Insulation was wrapped around the evaporator and adiabatic portions to reduce the heat leaks from the heat pipe to the ambient.

3.6 Empirical procedure

This study examines the influence of graphene and Al_2O_3 nanofluids on heat pipe performance under varying tilt angles and heat loads, employing forced-convection cooling with a fan. The heat pipe was inclined at three tilt angles: 0° (Horizontal), 60°, and 90° (Vertical). The condenser section was maintained above the HP evaporator for all inclined positions [21, 24]. Al_2O_3 -graphene water nanofluid, and water were used as the working fluids for the heat pipe, in which water readings were considered as the baseline reading for the experiment. The heat flux input was varied from 10 W to 20 W in steps of 5 W. The mica heater's limiting operating temperature (160 ℃) was considered the limiting factor for heat input. A data logger temperature scanner recorded all temperature readings at the 10-minute mark. The detailed specifications of the heat pipe and experimental setup used in this study are summarized in Table 5.

Table 5. Heat pipe specifications

Criterions	Description
Heat pipe material	Copper
Base working fluid	Al_2O_3 -graphene water nanofluid
Type of wick	Copper Screen mesh
Size of wick	40 mesh (1 layer)
Wire mesh diameter	0.15 mm
Ratio for filling	50%
Length of evaporator section	50 mm
Length of adiabatic section	200 mm
Length of condenser section	150 mm
Total length of heat pipe	400 mm
Total width of the heat pipe	22 mm
Thickness of heat pipe	3 mm

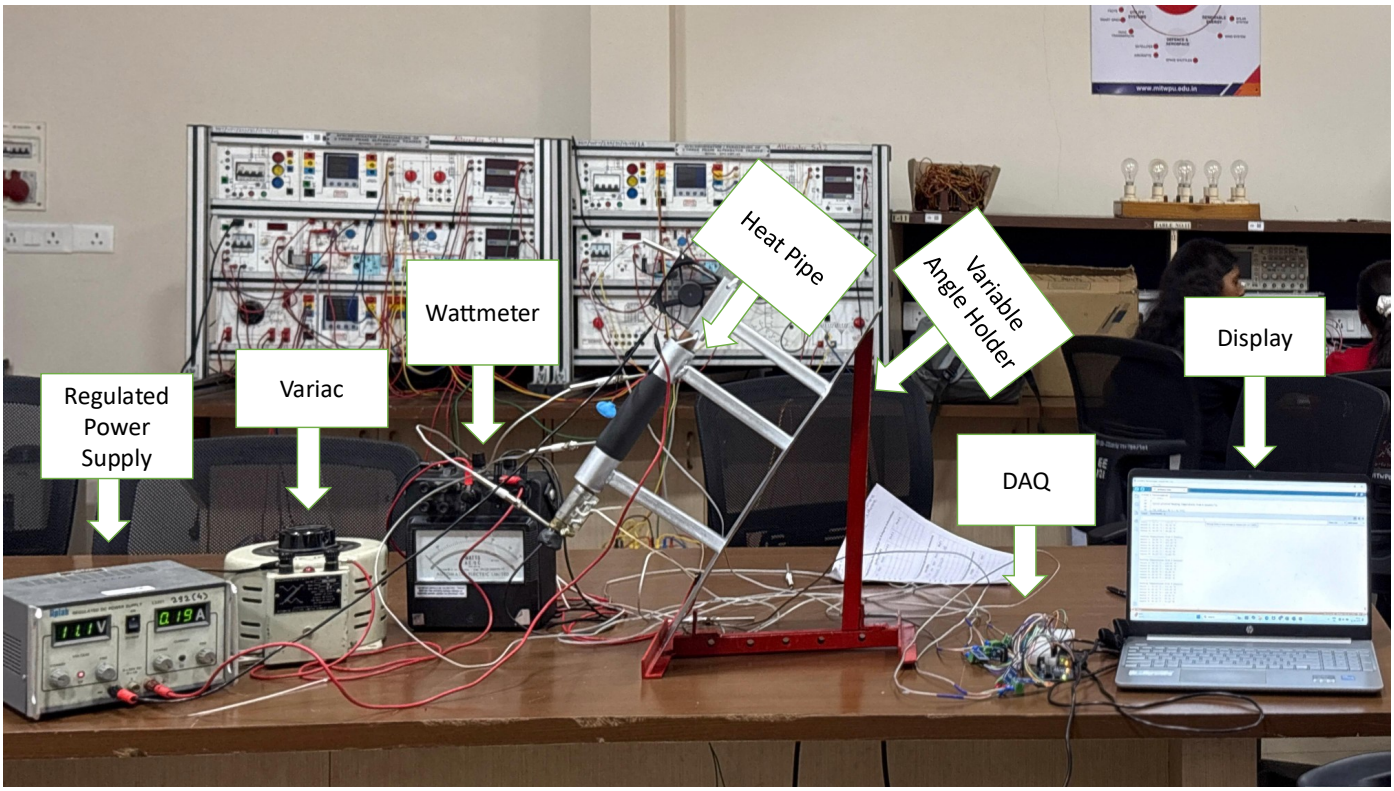

Figure 2. Experimental setup

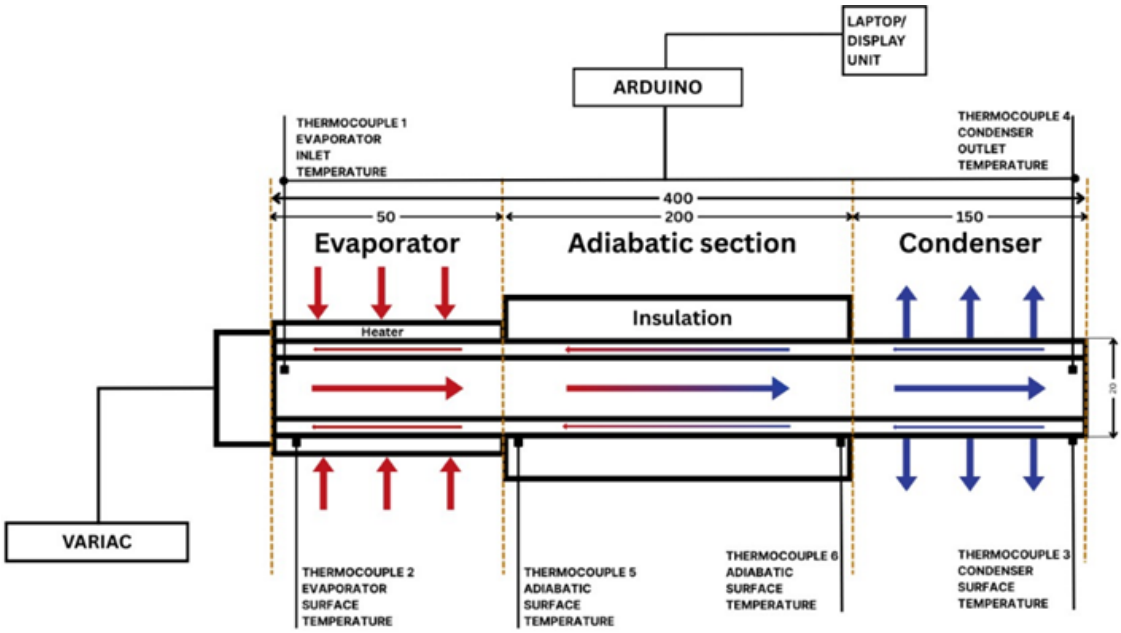

Figure 3. Schematic diagram of heat pipe

4. DATA REDUCTION

At each incremental value of the input power Q, the dissipated wall heat flux of the evaporator section, Qe, and the evaporator section heat transfer coefficient, He, are computed from the measured values and the averaged values of the thermocouple readings from the following set of equations;

1. Heat transfer coefficient at evaporator section

$$He = Qe/Te\text{-}Ta \tag{8}$$

where, Qe = Q/Ae.

The heat input, denoted as Qe, is the energy supplied to the evaporator. The evaporator section has a surface area, denoted Ae, that plays a key role in heat transfer. The mean temperature at the evaporator section is labelled Te, while the mean temperature at the adiabatic section is Ta. In this scenario, we assume no heat loss, implying the system is perfectly insulated. This setup ensures that the input heat and the temperatures at the various sections solely determine the energy flow.

2. Thermal resistance of the nano-fluid

$$R = (T1 - T3)/ Q \tag{9}$$

T1 = Evaporator Inlet Temperature
T3 = Condenser Outlet Temperature
Q = Heat Input

here, the thermal resistance of the heat pipe is considered the primary criterion for selecting the appropriate heat pipe for a given inclination angle across varying volume percentages.

5. RESULTS AND DISCUSSIONS

Heat pipe with Al_2O_3-Graphene HNF at 4%–3%, 3%–2%, and 6%–3% volume percentage, and water were investigated over a heat input range from 10 W to 20 W, with a step of 5 W. We have discussed the effect of the inclination angle on the heat-transfer coefficient at varying heat loads on the evaporator temperature, the total thermal resistance, and the percentage decrease in thermal resistance. To evaluate the optimal volume percentage of hybrid nano fluid and inclination angle at various heat loads.

5.1 Effect of inclination angle on the performance of the heat pipe

This preliminary graph illustrates how thermal resistance varies with inclination angle, from 0° to 60° and then to 90° at various heat loads for different hybrid nanofluids. One key observation was made for the 4% Al_2O_3 + 3% Graphene hybrid nanofluid at a heat load of 10 W: as the inclination increased from 0° (horizontal) to 60°, the thermal resistance decreased by approximately 29%. This significant decrement confirms the importance of the inclination angle for heat pipe performance, establishing the fundamental principle that gravity-based heat pipes perform better than those in a horizontal position. An intriguing observation is that as the heat load increased, the decrease in thermal resistance became pronounced. This further confirms that, with a larger inclination angle, such as 60°, the advantages are amplified at high heat loads. In the case of the second hybrid nanofluid consisting of 3% Al_2O_3 and 2% Graphene, the decrement in thermal resistance was 25% at a heat load of 10 W when the position was moved from 0° to 60°. Moreover, for heat loads of 15 W and 20 W, the decrement further decreased to 52%. As before, this confirms that with a high heat load, the advantages of inclination are amplified.

As shown in Figure 4, on the other hand, for both of the previously mentioned hybrid nanofluids-4% Al_2O_3 + 3% Graphene and 3% Al_2O_3 + 2% Graphene, at the inclination of 90°, the thermal resistance reduction was relatively small, with a maximum drop of only about 18%. This indicates that the optimal angle is 60° to enhance performance. At this angle, it achieves an optimal balance between gravitational assistance and capillary action within the wick. However, when

investigating the 6% Al_2O_3 + 3% Graphene hybrid nanofluid, we observed minimal reduction in thermal resistance, approximately 5%–9%, even when the inclination was varied from 0° to 60°. This negligible variation indicates that the heat pipe's performance was degraded by agglomeration at a nanoparticle concentration of nearly 10% by volume. This most likely caused clogging within the wick structure and, consequently, degraded the heat pipe's functionality.

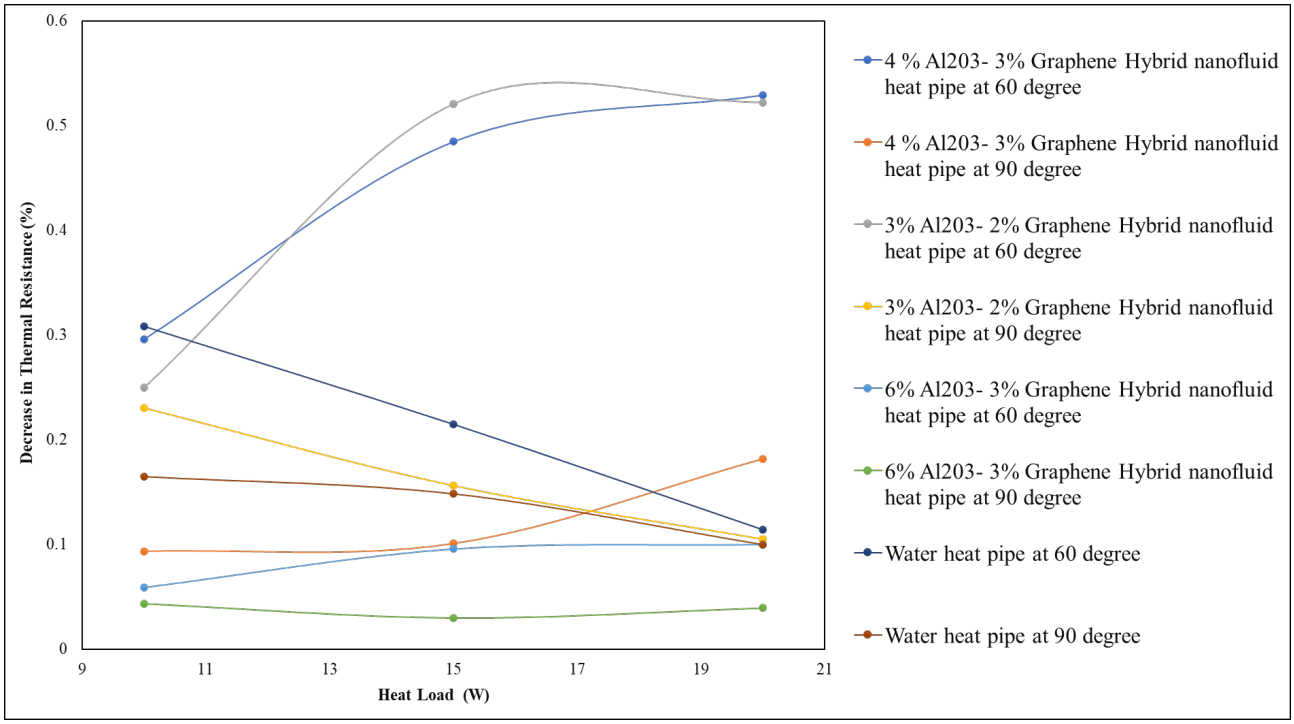

Figure 4. Decrease in thermal resistance for different inclination angles

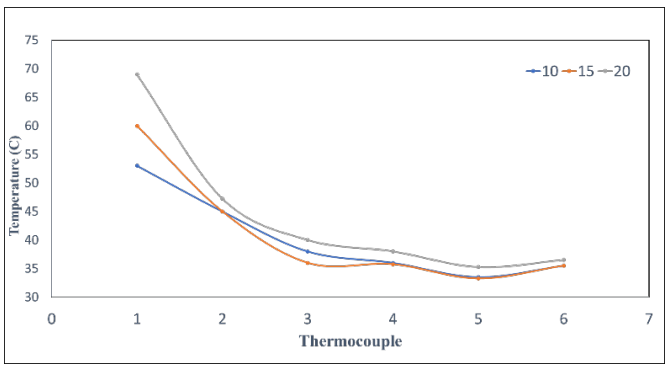

Figure 5. Temperature across the heat pipe 4% Al_2O_3 + 3% graphene hybrid nanofluid heat pipe at 60 °C

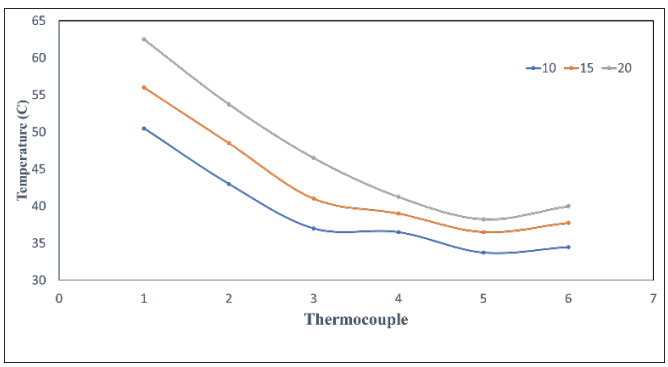

Figure 6. Temperature across the heat pipe 3% Al_2O_3 + 2% graphene hybrid nanofluid heat pipe at 60 °C

Therefore, this data suggests that when there's little to no change in thermal resistance with an increasing inclination angle, the observed heat transfer improvement is driven by the intrinsic thermal conductivity of the nanofluid itself, rather than any gravitational effects. As shown in Figure 5 and Figure 6, in contrast, the performance gains with the 4% Al_2O_3 + 3% Graphene and 3% Al_2O_3 + 2% Graphene nanofluids were clearly influenced by both enhanced thermal conductivity and favourable orientation, indicating a synergistic effect of the optimized fluid composition and inclination. More interestingly, even water outperformed the 6% Al_2O_3 + 3% Graphene nanofluid in terms of the percentage reduction in thermal resistance across all tested inclination angles. This further supports the conclusion that excessively high nanoparticle concentrations may lead to practical failures in the heat pipe system.

5.2 Effect of inclination angle on evaporator heat transfer coefficient at varying heat loads

With a heat load of 2411.963 W/m², the heat pipe using a 4% Al_2O_3-3% graphene hybrid nanofluid exhibited a heat transfer coefficient of 344.57 W/m²·K at 0° inclination. As the heat pipe was inclined at 60°, the heat transfer coefficient increased to 459.42 W/m²·K, a 33% increase relative to the value at 0°. For 90° inclination, the coefficient marginally reduced to 438.54 W/m²·K, but a 27% increase was still observed compared to the value at 0°. As the heat load was increased to 3617.945 W/m², the heat transfer coefficient at 0° increased to 401.99 W/m²·K. For a 60° inclination, the coefficient again increased to 516.84 W/m²·K, a 28.6% increase relative to 0°. At 90°, the coefficient was 499.03 W/m²·K, a 24% increment relative to the value at 0°. For the highest heat load of 4823.927 W/m², the heat transfer coefficient at 0° increased substantially to 665.37 W/m²·K. At

60°, the coefficient increased slightly to 689.13 W/m²·K, representing a 3.6% increase. At 90°, the coefficient slightly reduced to 669.99 W/m²·K, although a 0.7% increase was observed compared to the value at 0°.

As shown in Figure 7, for the 4% Al_2O_3-3% graphene hybrid nanofluid at a heat load of 2411.963 W/m², the increase in the heat transfer coefficient was 33% when the inclination angle was increased from 60° to 90°. However, as the heat load rose to 4823.927 W/m², the increase in the heat transfer coefficient was substantially lower, at only 3.6%. This indicates that, beyond a certain point, the heat-transfer coefficient in the evaporator section is independent of the inclination angles.

For a heat load of 2411.963 W/m², the heat transfer coefficient of the 3% Al_2O_3 and 2% graphene hybrid nanofluid-filled heat pipe with 0° inclination was 332.68 W/m²K. When inclined at 60°, it increased to 401.99 W/m²·K, an increase of approximately 20.8%. At 90°, it decreased slightly to 385.91 W/m²·K, yet it increased by 15.99% relative to 0°. As the heat load was increased to 3617.945 W/m², the heat transfer coefficient at 0° increased to 391.12 W/m²·K. Upon inclining it to 60°, it increased to 482 W/m²·K, indicating a 23.23% improvement. At 90°, it decreased slightly to 452 W/m²·K, yet it was 15.58% higher than at 0°. For the highest possible heat load of 4823.927 W/m², the heat transfer coefficient at 0° increased to 643.19 W/m²·K. When inclined at 60°, it increased slightly to 665 W/m²·K, representing a 3.39% improvement. At 90°, it decreased to 643.19 W/m²·K, indicating no further increase relative to 0°.

The heat pipe with a 6% Al_2O_3- 3% graphene hybrid nanofluid, operating at a heat load of 2411.963 W/m², had a heat-transfer coefficient of 357.32 W/m²·K at a horizontal inclination of 0°. The coefficient increased to 438.54 W/m²·K at an inclination of 60°, representing a 22.7% increase. Subsequently, the inclination was increased to 90°, and the coefficient decreased to 419.47 W/m²·K, although it remained 17.4% higher than at 0°. For a heat load of 3617.945 W/m², the heat transfer coefficient for a 0° inclination was 397.58 W/m²·K. For an inclination of 60°, the coefficient increased to 499.03 W/m²·K, a 25.5% increase. Then, for a 90° inclination, the coefficient decreased to 466.83 W/m²·K, but it was still 17.3% higher. At the highest heat load of 4823.927 W/m², the heat transfer coefficient for a 0° inclination is 660.81 W/m²·K. The heat transfer coefficient at a 60° inclination increased to 684.24 W/m²·K, a 3.6% increase. However, at 90°, the heat transfer coefficient decreased to 622.44 W/m²K, which was still slightly higher than that at 0°, but indicated a reduced influence of inclination angle at higher heat loads.

When comparing 6% Al_2O_3 and 3% graphene hybrid nanofluid with water, the following results are encountered:

Heat load of 2411.963 W/m²: Both the hybrid nanofluid and water experience a rise in the heat transfer coefficient in the evaporator as the angle of inclination rises from 0° to 60°. For the hybrid nanofluid, the increment is 22.7%, whereas for water it is slightly higher at 24.7%. At a higher heat load of 4823.927 W/m², water showed an 11.8% increase in the heat-transfer coefficient as the inclination angle increased from 0° to 60°, whereas the hybrid nanofluid showed only a 3.6% increase.

This suggests that for the hybrid nanofluid, there is a saturation point at a particular heat load, beyond which further increases in heat load do not yield significant improvements in the heat transfer coefficient. At a heat load of 2411.963 W/m², the heat-transfer coefficient at the evaporator for water was 214.97 W/m²·K at a 0° inclination. Increasing the inclination to 60° increased the coefficient to 267.99 W/m²·K, representing approximately a 24.7% increase. At 90°, the coefficient was slightly lower at 260.75 W/m²·K, but still 21.3% higher than at 0°. When the heat load was increased to 3617.945 W/m², the heat transfer coefficient for water at 0° was 237.24 W/m²·K. At 60°, it increased to 278.30 W/m²·K, reflecting a 17.3% improvement. At 90°, the coefficient decreased slightly to 267.99 W/m²·K, remaining approximately 12.9% higher than at 0°. At the highest heat load of 4823.927 W/m², the heat-transfer coefficient at the evaporator for water at 0° was 253.89 W/m²·K. At 60°, the coefficient increased to 283.76 W/m²·K, representing an 11.8% improvement. At 90°, the coefficient decreased slightly to 271.77 W/m²·K but remained 7% higher than at the horizontal position.

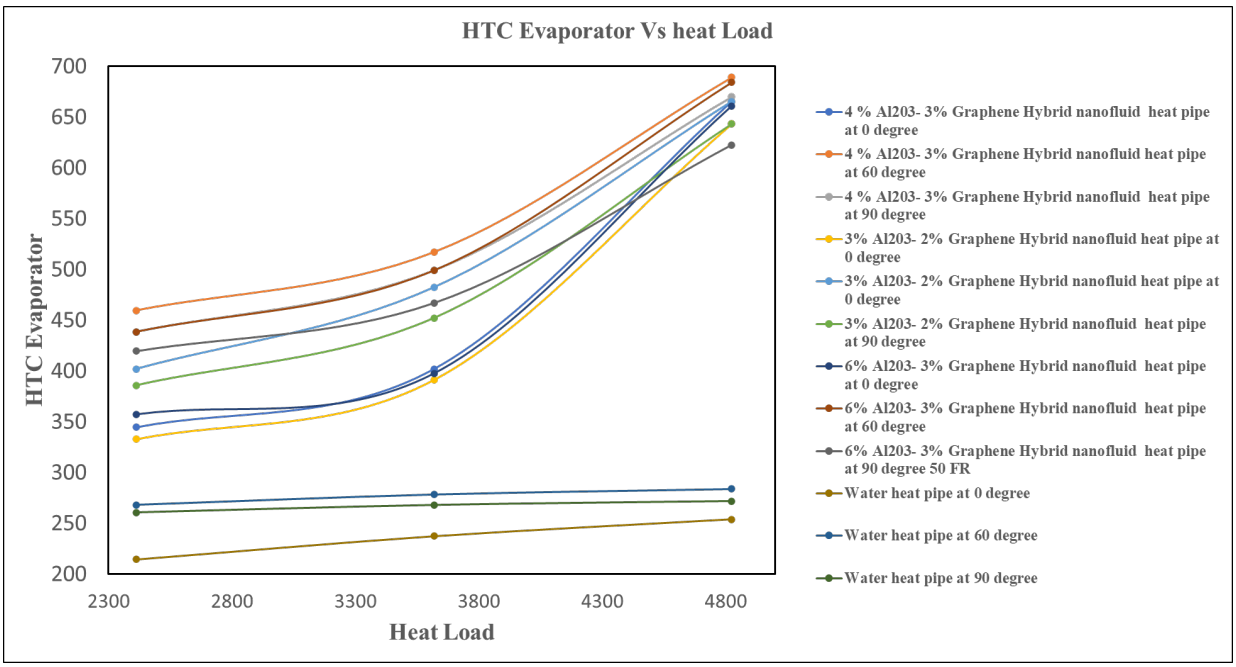

Figure 7. Heat transfer coefficient evaporator vs heat load

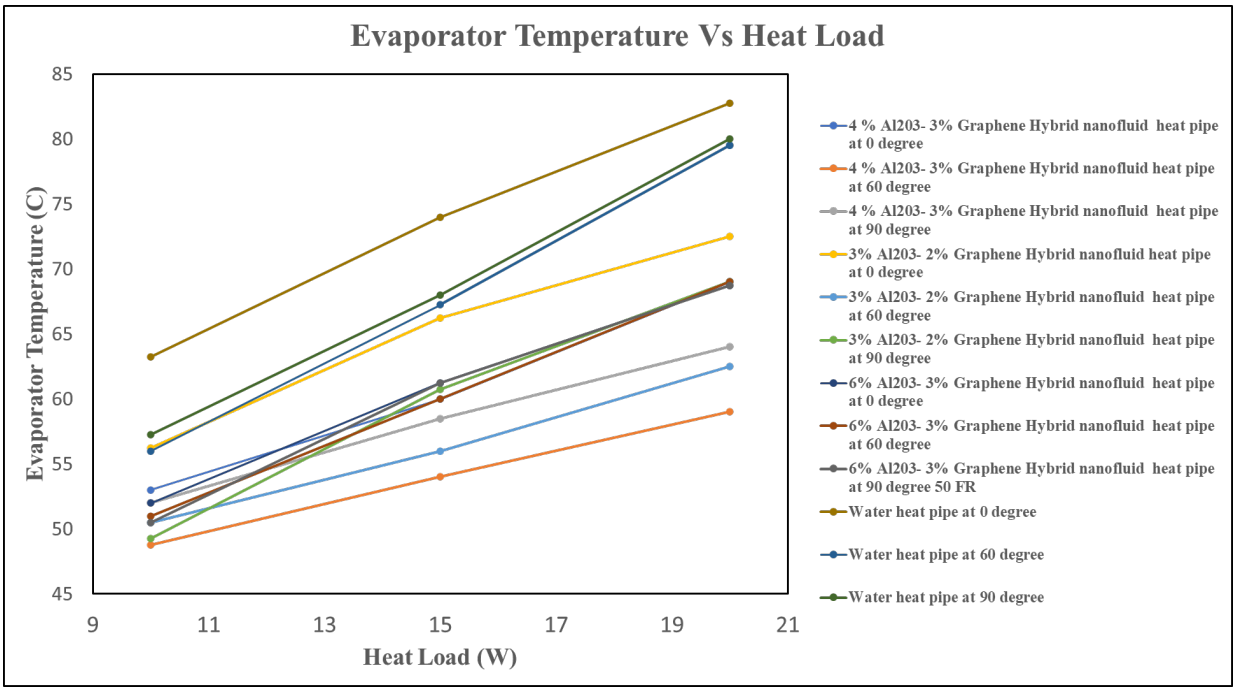

Figure 8. Evaporator temperature vs heat load

5.3 Effect of inclination angle on evaporator temperature at varying heat loads

The lowest evaporator temperature was observed for Al_2O_3-Graphene HNF at 4%–3% at a 60-degree inclination angle, whereas the highest temperature was observed for water at a 0-degree inclination angle. At a constant heat input of 10W and a hybrid nanofluid composition of 4% Al_2O_3 + 3% Graphene, we observed that the evaporator temperature of the heat pipe varied significantly with the inclination angle. Figure 8 shows the effect of inclination angle on the evaporator temperature at different heat loads.

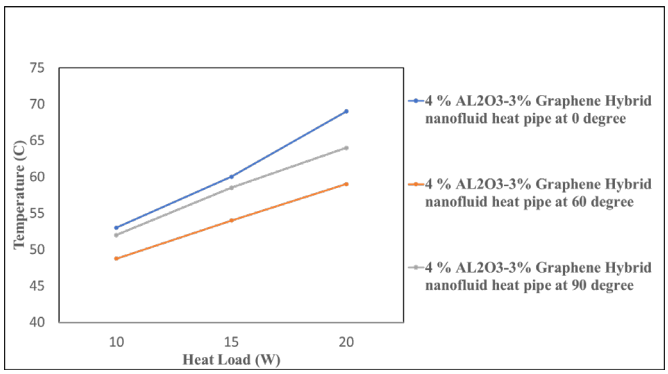

Figure 9. Evaporator temperature variation for 4% Al_2O_3 + 3% graphene hybrid nanofluid heat pipe

As shown in Figure 9, when the heat pipe was in the horizontal position (0° inclination angle), the evaporator temperature reached 53 °C. However, when the heat pipe was further inclined to 60°, the evaporator temperature decreased substantially, dropping to 48.75 °C. This showed an apparent 8.02% decrease in comparison to the horizontal orientation. This improvement is attributed to enhanced gravitational assistance during the condensate's return to the evaporator, thereby improving thermal performance. At a vertical angle of 90°, the evaporator temperature increased slightly to 52 °C, representing a 6.67% increase relative to the 60° position and a 1.89% decrease relative to the horizontal position. The result obtained by Zhang et al. [15] proves that the effect of gravity exists in the thermal performance, because the processes of evaporation and condensation of the working fluid affect each other, thereby causing a reduction in the rate of heat transfer between the evaporator and the condenser at an inclination angle of 90°. For a heat input of 15 W, the trend reported above for the change in evaporator temperature with the inclination angle was reproduced.

In this case, when the heat pipe was held at a fixed angle of 0°, the evaporator temperature was measured to be 60 °C. However, when it was raised to an inclined position of 60°, the temperature decreased to 54 °C, corresponding to a 10% decrease. With successive increments in the inclination angle to 90°, the temperature increased to 58.5 °C, an 8.33% increase relative to 60°. Notably, this was still lower than the temperature recorded at zero degrees. When the heat load was increased to 20W, this trend continued. The evaporator temperatures were highest at 60 °C. When the angle was increased to 60°, the temperature decreased to 59 °C. This was attributed to a 14.49% reduction. However, when this position was raised to 90°, temperatures went higher to 64 °C. This was attributed to an 8.47% increase. Still, this was lower than the temperature at 0 °C. The smallest possible temperature difference was observed when the inclination angle increased from 50° to 70°, as reported by Zhang et al. [14].

The optimal inclination angle for Heat Pipes will be further discussed in this study, consistent with prior studies. An interesting trend was identified: as the heat load increases, the percentage difference in thermal resistance becomes larger for the same inclination angle. For example, at an inclination angle of 60°, the thermal resistance decreased by 8.02% at a 10 W heat load; however, as the heat load increased to 20 W, the decrease was 14.49%.

Likewise, for a heat flux of 10W, the evaporator temperature for the 3% Al_2O_3-2% Graphene hybrid nanofluid exhibited a similar trend with the inclination angle. At an angle of 0°, the temperature was measured to be 56.25 °C. Subsequently, as the incline angle increased to 60°, the

temperature decreased to 50.5 ℃, indicating a 10.23% decrease. Furthermore, as the incline angle increased to 90°, the temperature decreased to 49.25 ℃, suggesting a 2.48% reduction relative to the 60° case and a total decrease of 12.46% relative to the 0° case.

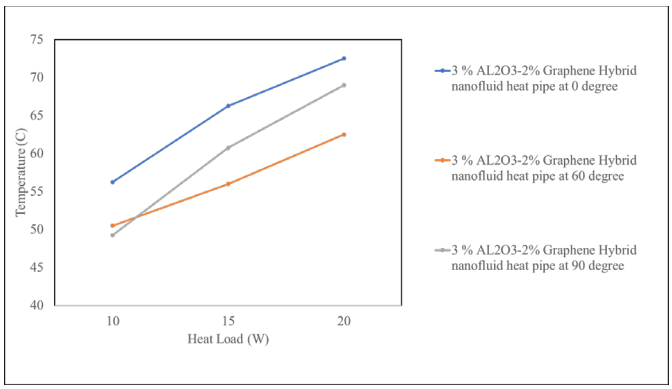

Figure 10. Evaporator temperature variation for 3% Al_2O_3 + 2% graphene hybrid nanofluid heat pipe

For a heat load of 15 W, as shown in Figure 10, the trend was the same for the 3% Al_2O_3-2% Graphene hybrid nanofluid. The evaporator temperature at 0° inclination was 66.25 ℃. When the heat pipe was inclined by 60°, the temperature decreased to 56 ℃, corresponding to a 15.47% reduction. The temperature further elevated to 60.75 ℃ at an inclination of 90°, an increase of 8.48% above the 60° position but an 8.30% reduction relative to the temperature at 0° inclination. However, when the heat load was increased to 20 W, the trend persisted for the 3% Al_2O_3-2% Graphene hybrid nanofluid. The temperature at the evaporator head for the heat pipe at 0° inclination was 72.5 ℃. However, upon inclining the heat pipe by an additional 60°, the temperature decreased to 62.5 ℃, indicating a 13.79% reduction. However, at an additional inclination of 90°, the temperature increased to 69 ℃, an improvement of 10.4% over the temperature at the heat pipe at 60° but a reduction of 4.83% relative to the temperature at the heat pipe at 0° inclination. As observed earlier, the thermal resistance under a 10W heat load decreased by 10.23% at an angle of 60°, and under an additional 20W heat load, the reduction increased to 13.79%.

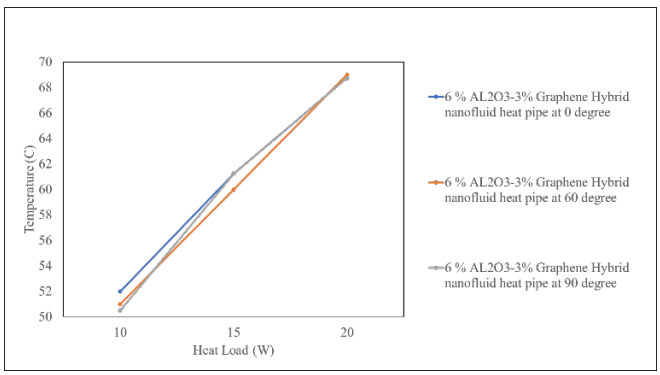

Figure 11. Evaporator temperature variation for 6% Al_2O_3 + 3% graphene hybrid nanofluid heat pipe

As shown in Figure 11, for the 6% Al_2O_3-3% Graphene hybrid nanofluid at a heat load of 10 W, the evaporator temperature decreases as the inclination angle increases. At 0°, the temperature was 52 ℃. Upon inclining it to 60°, a minute reduction to 51 ℃ was observed, corresponding to a 1.92% decrease. Furthermore, when it was placed vertically at 90°, the temperature decreased to 50.5 ℃, indicating a 0.98% reduction relative to 60° and a cumulative decline of 2.88% relative to 0°. For 15 W, however, it not only became minute but also exhibited a slightly decreasing pattern. As expected, it started at 61.25 ℃ at 0°, then slightly reduced to 60 ℃ at 60°, indicating a 2.04% improvement. As expected, even at 90°, it returned to 61.25 ℃, indicating performance comparable to that at 0°. Thus, it is clear that at a 15 W heat load, optimal performance was achieved at 60°. For 20 W, though, it became even more minute. As expected, at 0° it started at 68.75 ℃, increased to 69 ℃ at 60°, and then decreased slightly to 68.75 ℃ at 90°. As observed, it became flat, implying that at higher heat loads, even minute variations due to angle become irrelevant for the 3% Graphene hybrid nanofluid.

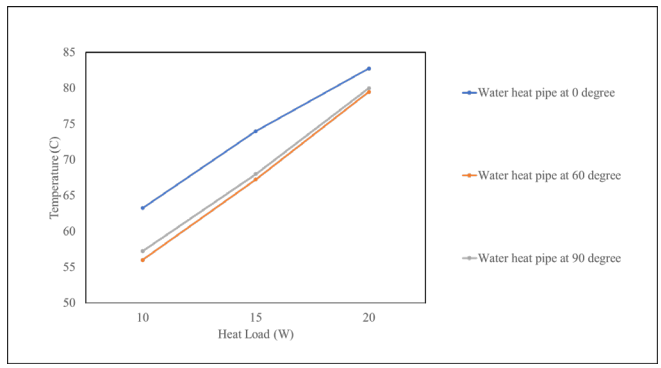

Figure 12. Evaporator temperature variation for water heat pipe

For the water heat pipe, as shown in Figure 12, the evaporator temperature varied with position, particularly at low heating power. At 10 W, the temperature was 63.25 ℃ when the position was maintained at 0°. When the position was changed to 60°, the temperature decreased to 56 ℃, indicating a substantial increase in the heat-transfer rate. Furthermore, when the position was set to 90°, the temperature increased slightly to 57.25 ℃, but it remained much lower than at the 0° position. A similar trend was observed at 15 W, where the temperature began at 74 ℃ at 0°, decreased to 67.25 ℃ at 60°, and then increased slightly to 68 ℃ at 90°. It can thus be inferred that the most favorable position was 60°. At 20 W, the changes were more subtle. The evaporator temperature decreased from 82.75 ℃ at 0° to 79.5 ℃ at 60°, then increased to 80 ℃ at 90° [9].

It can be observed that, unlike the 4% Al_2O_3 + 3% Graphene and 3% Al_2O_3 + 2% Graphene hybrid nanofluids— where a significant reduction in evaporator temperature was seen with increasing inclination angles—the 6% Al_2O_3 + 3% Graphene hybrid nanofluid showed minimal to no change in evaporator temperature across different orientations. This indicates that the beneficial effect of gravity-assisted inclination was not effectively realized in this case. A likely explanation for this behavior is the nanofluid's tendency to agglomerate at such a high concentration. Nanofluid agglomeration occurs due to clumping between particles due to the van der Waals force and weakening of brown motion in a nanofluid. Agglomeration reduces the degree of homogeneity in the nanofluid, causing the particles to settle at the bottom and making the nanofluid appear clear at the top [23]. The dense particle loading may have led to clogging within the wick structure, thereby

hindering capillary action, which is essential for effective heat pipe operation. This blockage would disrupt the return flow of the working fluid, weakening the heat pipe effect and resulting in stagnant thermal performance regardless of the inclination angle. However, despite this issue, the evaporator temperatures at all orientations for the 6% Al_2O_3 + 3% Graphene nanofluid were still lower compared to those of the 3% Al_2O_3 + 2% Graphene nanofluid and pure water. This can be attributed to the inherently higher thermal conductivity of the 6% Al_2O_3 + 3% Graphene hybrid nanofluid, which allows better heat absorption and transfer even in the absence of optimal fluid circulation within the pipe.

5.4 Effect of inclination angle on total thermal resistance

As shown in Figure 13, The lowest evaporator thermal resistance was observed for Al_2O_3-Graphene HNF at 4%–3% at a 60-degree inclination angle, whereas the highest thermal resistance was observed for water at a 0-degree inclination angle.

At a constant heat input of 10 W, as shown in Figure 14, and a hybrid nanofluid composition of 4% Al_2O_3 + 3% Graphene, we observed that the heat pipe's evaporator temperature varied significantly with the inclination angle. At a heat load of 10 W, the thermal resistance of the heat pipe using 4% Al_2O_3 + 3% Graphene hybrid nanofluid was measured to be 1.75 C/W at a 0° inclination angle. As the inclination increased to 60°, the thermal resistance decreased to 1.35 C/W, representing a 22.86% decrease. When the angle was increased to 90°, the thermal resistance was 1.6 C/W, representing a minor reduction of approximately 8.57% relative to the 0° position. At a heat input of 15 W, the thermal resistance of the heat pipe using a 4% Al_2O_3-3% Graphene hybrid nanofluid was 1.633 C/W at a 0° inclination angle. By increasing the inclination to 60°, the thermal resistance decreased noticeably to 1.1 C/W, corresponding to a 32.65% reduction. It recorded 1.4833 kW at 90°, with a minor decrease of approximately 9.16% relative to the horizontal position. The measured thermal resistance of the heat pipe filled with a hybrid nanofluid containing 4% Al_2O_3 and 3% Graphene, when positioned horizontally (0° inclination), was 1.625 C/W at a heat load of 20 W. The thermal resistance decreased to 1.0625 C/W as the inclination angle increased to 60°, representing a reduction of approximately 34.62%. At the 90° inclination, the thermal resistance was 1.375 C/W, representing a 15.38% decrease relative to the 0° position.

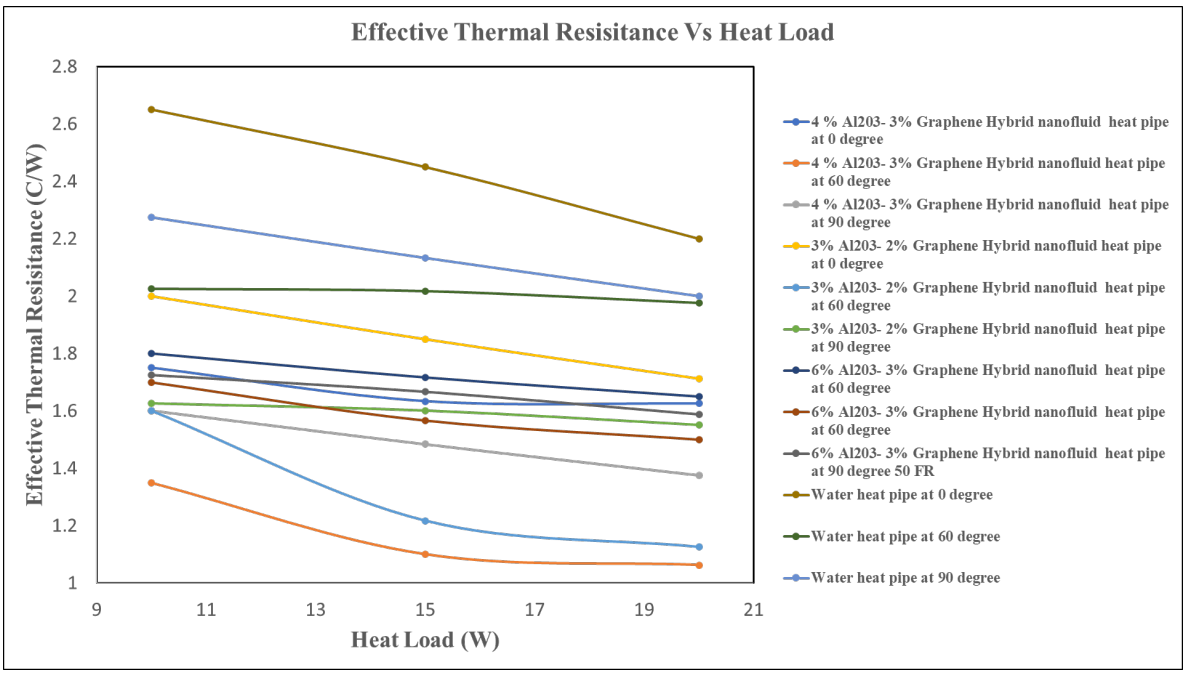

Figure 13. Effective thermal resistance vs heat load

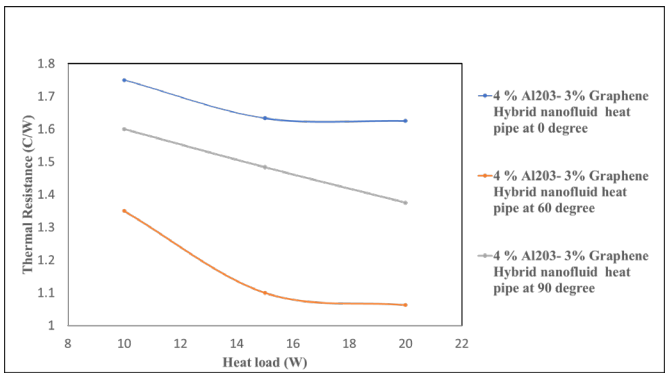

Figure 14. Thermal resistance variation for 4% Al_2O_3 + 3% graphene hybrid nanofluid heat pipe

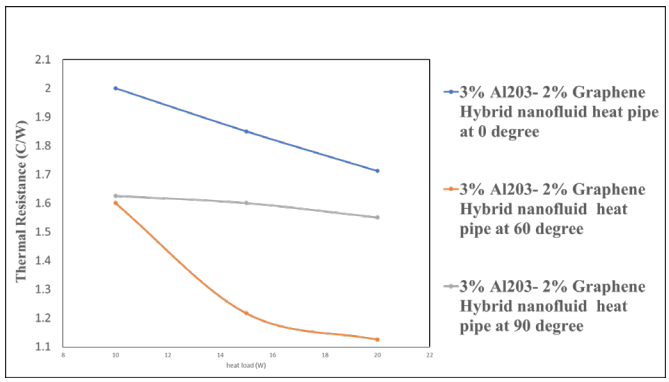

Figure 15. Thermal resistance variation for 3% Al_2O_3 + 2% graphene hybrid nanofluid heat pipe

A trend was also observed: as the heat load increases, the thermal resistance decreases by a larger percentage for the same inclination angle. As an example, the thermal resistance was reduced by 22.86%. at an inclination of 60° and for a heat load of 10W, which increased to 34.62%.

For a heating power of 10 W, as shown in Figure 15, the thermal resistance of the heat pipe filled with a 3% Al_2O_3-2% Graphene hybrid nanofluid in the horizontal (0°) position was measured to be 2 C/W. However, with an increase in orientation to 60°, the power output decreased to 1.6 kW, a 20% reduction. Further increasing it to 90° slightly increased it to 1.625 C/W, which was still an 18.75% reduction. When the heating power was increased to 15 W, the temperature rise was 1.85 C/W at 0°. This decreased to 1.21 C/W at 60° (34.59% reduction) and to 1.6 C/W at 90° (approximately 13.51% reduction). For an even higher heating power of 20 W, it measured 1.71 C/W at 0°. This further decreased to 1.125 C/W at 60° (34.21% reduction) and to 1.55 C/W at 90° (approximately 9.36% lower than in the horizontal position).

At a heat load of 10 W, the thermal resistance of the heat pipe was measured to a heat load of 10 W, as shown in Figure 16. The heat pipe with the 6% Al_2O_3-3% Graphene hybrid nanofluid measured 1.8 C/W at 0°, which was progressively lowered at 60° to 1.7 C/W—a steep decrease of 5.56%. However, at 90°, the reading was 1.725 kW, representing a 4.17% decline relative to the previous position. When the heat load was increased to 15 W, the reading at 0° was 1.7166 C/W. This further declined to 1.5667 kW at 60°, representing an 8.73% decrease, whereas at 90° the value was 1.66 kW, 3.3% lower than the initial value. At an even higher heat load of 20 W, the reading at 0° was 1.65 C/W. This decreased at 60° to 1.5 C/W (9.09%), whereas at 90° the reading was 1.5875 C/W (3.78%).

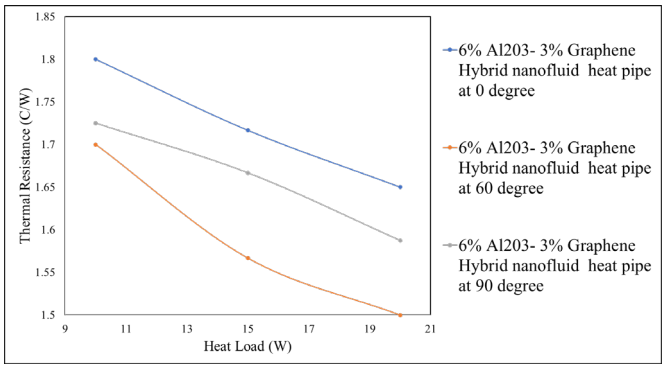

Figure 16. Thermal resistance variation for 6% Al_2O_3 + 3% graphene hybrid nanofluid heat pipe

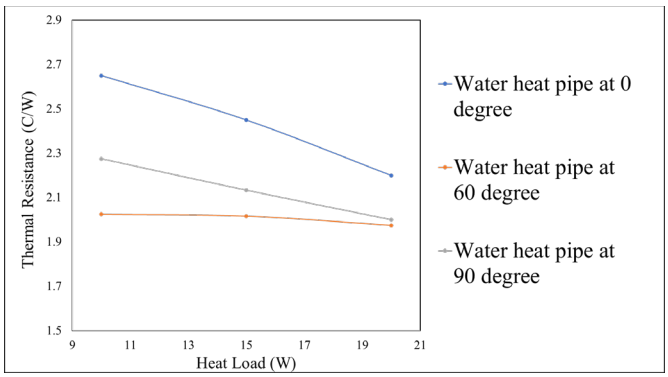

Figure 17. Thermal resistance variation for water heat pipe

Interestingly, as shown in Figure 17, for 6% Al_2O_3- 3% Graphene hybrid nanofluids, the reduction in thermal resistance percentage with increasing inclination angle was relatively small. At a heat load of 10 W, an increase in the inclination angle from 0° to 60° caused a reduction of 5.56%, whereas an increase from 0° to 90° caused a decrease of 9.09%. In comparison, water exhibited a more significant change under similar conditions—showing a 23.81% reduction in thermal resistance at 10 W when moving from 0° to 60°, and a 10.23% reduction at 20 W for the exact inclination change. This highlights the relatively limited sensitivity of the 6% Al_2O_3 and 3% graphene nanofluids to changes in inclination angle, particularly compared with water.

At a heat load of 10 W, the thermal resistance of the heat pipe with water as the working fluid was 2.65 C/W when horizontally oriented (0° inclination). As the inclination angle increased.

6. CONCLUSIONS

The thermal performance of heat pipes containing varying volume fractions of Al_2O_3-graphene hybrid nanofluids was experimentally investigated under varying heat loads and tilt angles. Based on the present experimental work, the following inferences are made:

1. The thermal behaviour of the heat pipe was seen to be the best for 4% Al_2O_3 + 3% Graphene hybrid nanofluid in comparison to other volume concentrations of hybrid nanofluid and water.
2. The effective thermal resistance decreased with heat load for all three volume concentrations of hybrid nanofluid considered in this study, with the highest decrease in 4% Al_2O_3 + 3% Graphene hybrid nanofluid at a 60-degree inclination angle and 20 W heat load.
3. The 60-degree inclination angle outperformed 0-degree and 90-degree inclination angles for all considered cases because gravity has a significant role in the thermal performance as the processes of evaporation and condensation of working fluid interfere with each other, which decelerates the heat transfer rate between evaporator and condenser under an inclination angle of 90°.
4. Lowest evaporator temperature was witnessed for Al2O3-Graphene HNF at 4%–3% at 60-degree inclination angle, and the highest temperature was seen for water at 0-degree inclination angle. Due to optimal thermal conductivity enhancement and gravity-assisted inclination angle.
5. The effect of tilt angle on 6% Al_2O_3 and 3% Graphene hybrid nanofluid was seen to be the least in comparison to other Volume concentrations, as the heat pipe's performance was seen to be negatively affected, likely due to agglomeration at such a high nanoparticle concentration (nearly 10% by volume). It is suspected that this caused clogging within the wick structure, ultimately compromising the heat pipe's functionality even at gravity-assisted inclination angles and higher heat loads.

Future studies can then focus on optimising the compositions and parameters of hybrid nanofluids for specific cooling requirements of electronic devices, such as power-electronics cooling, electric-vehicle module coolers, and small computing systems. Although this work examined heat loads of 10 W, 15 W, and 20 W and observed a decrease in thermal

resistance with increasing heat rate, studies covering higher heat loads are necessary to ascertain real-world operating limits and the onset of evaporator dryout during transient periods. Similarly, although this work tested samples at 0°, 60°, and 90° inclinations, studies covering intermediate inclination angles are required to develop expertise and predict performance under gravity-assisted conditions in real-world environments, where perfectly aligned conditions are rarely possible. Further studies regarding stability and cost-performance trade-offs are required for developing these heat pipes based on hybrid nanofluids into real-world commercial products for appropriate heat management necessities.

REFERENCES

[1] Mathew, J., Krishnan, S. (2021). A review on transient thermal management of electronic devices. Journal of Electronic Packaging, 144(1): 010801. https://doi.org/10.1115/1.4050002

[2] Bumataria, R.K., Chavda, N.K., Panchal, H. (2019). Current research aspects in mono and hybrid nanofluid based heat pipe technologies. Heliyon, 5(5): e01627. https://doi.org/10.1016/j.heliyon.2019.e01627

[3] Septiadi, W.N., Trisnadewi, I.A.N.T., Putra, N., Setyawan, I. (2018). Synthesis of hybrid nanofluid with two-step method. E3S Web of Conferences, 67: 03057. https://doi.org/10.1051/e3sconf/20186703057

[4] Faghri, A. (2014). Heat pipes: Review, opportunities and challenges. Frontiers in Heat Pipes, 5(1). https://doi.org/10.5098/fhp.5.1

[5] Han, H., Cui, X., Zhu, Y., Sun, S. (2014). A comparative study of the behavior of working fluids and their properties on the performance of pulsating heat pipes (PHP). International Journal of Thermal Sciences, 82(1): 138-147. https://doi.org/10.1016/j.ijthermalsci.2014.04.003

[6] Mozumder, A.K., Akon, A.F., Chowdhury, H., Banik, S.C. (2010). Performance of heat pipe for different working fluids and fill ratios. Journal of Mechanical Engineering, 41(2): 96-102. https://doi.org/10.3329/jme.v41i2.7473

[7] Parametthanuwat, T., Rittidech, S., Pattiya, A., Ding, Y., Witharana, S. (2011). Application of silver nanofluid containing oleic acid surfactant in a thermosyphon economizer. Nanoscale Research Letters, 6(1): 315. https://doi.org/10.1186/1556-276X-6-315

[8] Smrity, A.M.A., Yin, P. (2024). Design and performance evaluation of pulsating heat pipe using metallic nanoparticles based hybrid nanofluids. International Journal of Heat and Mass Transfer, 218: 124773. https://doi.org/10.1016/j.ijheatmasstransfer.2023.124773

[9] Zufar, M., Gunnasegaran, P., Kumar, H.M., Ng, K.C. (2020). Numerical and experimental investigations of hybrid nanofluids on pulsating heat pipe performance. International Journal of Heat and Mass Transfer, 146: 118887. https://doi.org/10.1016/j.ijheatmasstransfer.2019.118887

[10] Gonzalez, M.A. (2014). Experimental study of a pulsating heat pipe using nanofluid as a working fluid. Ph.D. thesis, Washington State University.

[11] Sadeghinezhad, E., Akhiani, A.R., Metselaar, H.S.C., Tahan Latibari, S., Mehrali, M., Mehrali, M. (2020). Parametric study on the thermal performance enhancement of a thermosyphon heat pipe using covalent functionalized graphene nanofluids. Applied Thermal Engineering, 175: 115385. https://doi.org/10.1016/j.applthermaleng.2020.115385

[12] Rama Narasimha, K., Sridhara, S.N., Rajagopal, M.S., Seetharamu, K.N. (2012). Influence of heat input, working fluid and evacuation level on the performance of pulsating heat pipe. Journal of Applied Fluid Mechanics, 5(2): 33-42. https://doi.org/10.36884/jafm.5.02.12165

[13] Mahdavi, M., Tiari, S., De Schampheleire, S., Qiu, S. (2018). Experimental study of the thermal characteristics of a heat pipe. Experimental Thermal and Fluid Science, 93: 292-304. https://doi.org/10.1016/j.expthermflusci.2018.01.003

[14] Zhang, B., He, Z., Wang, W., Wang, J., Mikulčić, H., Klemeš, J.J. (2022). Investigation on the thermal performance of flat-plate heat pipes with various working fluids under different inclination angles. Energy Reports, 8: 8017-8026. https://doi.org/10.1016/j.egyr.2022.06.040

[15] Veerasamy, A., Dharini, T. (2025). Effect of inclination angle on heat pipe (HP) performance with graphene nanofluids in electronic cooling applications. In Selected Proceedings of the 1st International Conference on Advanced Materials for Sustainable Innovation; IC-AMSI 2024; New Delhi; India, pp. 389-400. https://doi.org/10.1007/978-981-96-4492-6_30

[16] Allen, M.J., Sharifi, N., Faghri, A., Bergman, T.L. (2016). Effect of inclination angle during melting and solidification of a phase change material using a combined heat pipe-metal foam or foil configuration. International Journal of Heat and Mass Transfer, 80: 767-780. https://doi.org/10.1016/j.ijheatmasstransfer.2014.09.071

[17] Alammar, A.A., Al-Dadah, R.K., Mahmoud, S.M. (2016). Numerical investigation of effect of fill ratio and inclination angle on a thermosiphon heat pipe thermal performance. Applied Thermal Engineering, 108: 1055-1065. https://doi.org/10.1016/j.applthermaleng.2016.07.163

[18] Nazarimanesh, M., Yousefi, T., Ashjaee, M. (2015). Experimental study on the effects of inclination situation of the sintered heat pipe on its thermal performance. Experimental Thermal and Fluid Science, 68: 625-633. https://doi.org/10.1016/j.expthermflusci.2015.06.021

[19] Mwaba, M.G., Huang, X., Gu, J. (2006). Influence of wick characteristics on heat pipe performance. International Journal of Energy Research, 30(7): 489-499. https://doi.org/10.1002/er.1164

[20] Muneeshwaran, M., Srinivasan, G., Muthukumar, P., Wang, C.C. (2021). Role of hybrid-nanofluid in heat transfer enhancement – A review. International Communications in Heat and Mass Transfer, 125: 105341. https://doi.org/10.1016/j.icheatmasstransfer.2021.105341

[21] Cengal, Y. (2007). Heat and Mass Transfer: A Practical Approach. 3rd Ed, McGraw-Hill.

[22] Iverson, B.D., Davis, T.W., Garimella, S.V., North, M.T., Kang, S.S. (2007). Heat and mass transport in heat pipe wick structures. Journal of Thermophysics and Heat

Transfer, 21(2): 392-404. https://doi.org/10.2514/1.25809

[23] Peter, H., De Bock, J., Varanasi, K., Chamarthy, P., Deng, T., Kulkarni, A., Rush, B.M., Russ, B.A., Weaver, S.E., Gerner, F.M. (2008). Experimental investigation of micro/nano heat pipe wick structures. In Proceedings of the ASME 2008 International Mechanical Engineering Congress and Exposition. Volume 10: Heat Transfer, Fluid Flows, and Thermal Systems, Parts A, B, and C. Boston, Massachusetts, USA, pp. 991-996. https://doi.org/10.1115/IMECE2008-67288

NOMENCLATURE

Q_{out}	heat output, W
m	mass, kg
T_{out}	temperature at outlet, 0 ℃
T_{in}	temperature at inlet, 0 ℃
Q_{in}	heat input, W
T_{hot}	temperature at the hot side, 0 ℃
T_{cold}	temperature at the cold side, 0 ℃
d	diameter, m
Q_e	heat input at evaporator, W
T_e	average temperature of evaporator, ℃
$CapT_a$	average temperature of a diabetic, ℃
T_1	evaporator inlet temperature, ℃
T_4	adiabatic surface temperature, ℃

Greek symbols

ρ_{eff}	effective density, Kg·m^{-3}
ρ_b	base fluid density, kg·m^{-3}
ϕ_{hnp}	solid volume fraction
κ_{eff}	effective thermal conductivity, W/m·K
ϕ_{hnp}	volume percentage of hybrid nanoparticles
φ_{np}	volume percentage of nanoparticles
ρ_{np}	density of the Nanoparticle, Kg.m^{-3}
κ_b	thermal conductivity of Base fluid, W/m·K
κ_{np}	thermal conductivity of Nano particle, W/m·K
c_{peff}	adequate Specific heat of Nanofluid, J/kg·K
c_{pb}	specific heat of Base fluid, J/kg·K
c_{pnp}	specific heat of a Nano particle, J/kg·K
μ_{eff}	effective viscosity of nanofluid, N·S/m^2
μ_b	viscosity of the base fluid, N·s/m^2
ρ_{hnp}	density of hybrid nanoparticle, Kg·m^{-3}
ρ_{np1}	density of the Nanoparticle 1, Kg·m^{-3}
ρ_{np2}	density of the Nanoparticle 2, Kg·m^{-3}
ρ_{hnf}	density of hybrid nanofluid, Kg·m^{-3}
ϕ_{np1}	volume percentage of the Nano particle 1
ϕ_{np2}	volume percentage of the Nano particle 2
ρ_{bf}	density of base fluid, Kg·m^{-3}
Cp_{nf}	adequate specific heat of Nanofluid, J/kg·K
ϕ	effective volume percentage
ρ_{np}	density of the nanoparticle, Kg·m^{-3}
Cp_{bf}	specific heat of base fluid, J/kg·K
ρ_{nf}	density of Nanofluid, Kg·m^{-3}
Cp_{hnf}	specific heat of Hybrid Nanofluid, J/kg·K
Cp_{np1}	specific heat of nano particle 1, J/kg·K
Cp_{np2}	specific heat of nano particle 2, J/kg·K
k_{hnf}	thermal conductivity of Hybrid Nanofluid, W/m·K
k_{bf}	thermal conductivity of Base fluid, W/m·K
k_{np1}	thermal conductivity of Nano particle 1, W/m·K
k_{np2}	thermal conductivity of Nano particle 2, W/m·K